CHAPTER 9

CARBON FLUXES ACROSS REGIONS

Observational Constraints at Multiple Scales

BEVERLY E. LAW, DAVE TURNER, JOHN CAMPBELL,
MICHAEL LEFSKY, MICHAEL GUZY, OSBERT SUN,
STEVE VAN TUYL, AND WARREN COHEN

9.1 INTRODUCTION

Scaling biogeochemical processes to regions, continents, and the globe is critical for understanding feedbacks between the biosphere and atmosphere in the analysis of global change. This includes the effects of changing atmospheric carbon dioxide, climate, disturbances, and increasing nitrogen deposition from air pollution (Ehleringer and Field 1993, Vitousek et al. 1997). Quantification and uncertainty analysis of carbon pools and fluxes by terrestrial biota is needed to guide policy and management decisions. Unanswered questions include: (1) how and where is the terrestrial biosphere currently sequestering carbon? (2) how might forests be managed to maximize carbon sequestration? Managed carbon sequestration would have to be optimized within and among geographic regions with attention to how this might affect biodiversity and how to manage for the effects of "natural" disturbances on carbon storage and fluxes.

Processes in the terrestrial biosphere are dynamic and occur over a wide range of spatial and temporal scales. For example, net ecosystem production is the net effect of several large fluxes: photosynthetic uptake, and release of carbon dioxide (CO_2) by respiration from autotrophs (plants) and heterotrophs (e.g., microbial decomposition). Scales range from micrometers and microseconds (e.g., cellular processes such as photosynthesis) to kilometers and centuries (e.g., decomposition of recalcitrant pools of soil carbon) (Figure 9.1). Disturbance can have a significant effect on CO_2 loss to the atmosphere through decomposition of necromass such as that left from logging of forests, or pulses of CO_2 to the atmosphere from fire, and through manufacturing of forest products. Interannual variation in climate can influence photosynthesis and respiration differently such that net CO_2 uptake can

J. Wu, K.B. Jones, H. Li, and O.L. Loucks (eds.),
Scaling and Uncertainty Analysis in Ecology: Methods and Applications, 167–190.

change significantly. These factors complicate any simple scheme to quantify carbon storage and fluxes from ecosystems, yet it is important to know how disturbance and climate interact to affect biogeochemical processes for more informed management at the regional scale.

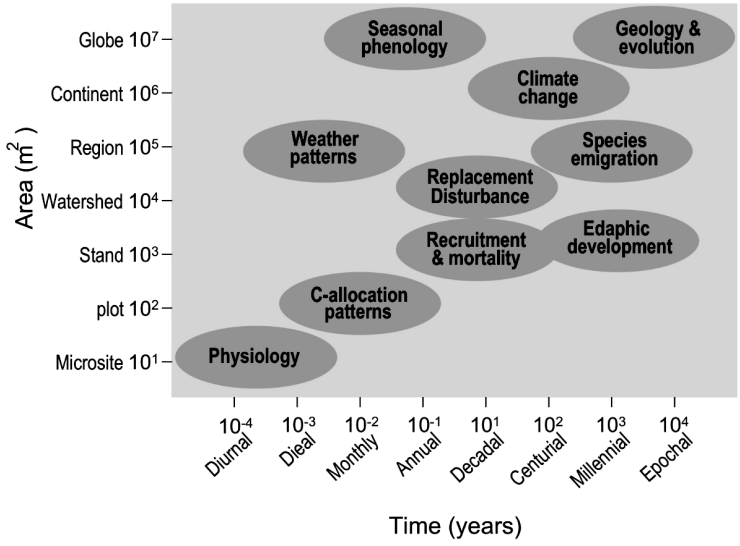

Figure 9.1. *Temporal and spatial scales of major processes affecting forest ecosystems.*

Scaling strategies in terrestrial processes often involve upscaling process data at a scale smaller than the scale of interest (e.g., leaf-level photosynthesis), and combining this information with structural and environmental data to quantify process rates at the scale of interest (Aber et al. 1993, Jarvis 1995, Wu and Li, Chapters 1 and 2). Such strategies take into account the feedbacks among components (e.g., atmosphere and vegetation), and linkages across scales (e.g., leaf-stand-landscape), and require that models are used and tested at each scale.

In this chapter, we demonstrate an approach to using field observations, remote sensing tools, and a biogeochemistry model (Biome-BGC) in a spatially nested hierarchy (Wu 1999) to improve predictions of carbon pools, productivity, and net ecosystem production (NEP) for every square kilometer of forests in a region. We examine uncertainty in a variety of ways for the different levels of data analysis.

9.2 ISSUES IN SCALING ECOSYSTEM PROCESSES

The interaction of processes operating at different spatial and temporal scales is one of the greatest challenges to regional estimates of biogeochemical processes. At any scale there is heterogeneity in types and rates of processes. For example, photosynthetic rates vary within a tree canopy (Reich et al. 1997). At larger scales,

the rates vary among different developmental stages of a given tree species as an indirect result of disturbance, and among different plant functional groups or biomes. Field observations are necessarily limited in scope, and logistical considerations make it infeasible to measure everything everywhere all of the time. Moreover, we simply do not understand some processes (e.g., respiration, carbon allocation within plant) as well as we understand others (e.g., photosynthesis). Simple aggregation and extrapolation schemes to larger spatial and longer temporal scales using field observations miss the critical role of feedbacks, which is an essential feature of scaling (Jarvis 1995, Wu and Li, Chapter 2).

Scientists have studied ecological systems for decades through observational studies, experiments, and development of models that incorporate their understanding of ecosystem function. Process models can be used to extend knowledge across time and space and to test hypotheses about coupling of processes and responses to environmental conditions. Considerable efforts have been expended to develop biogeochemical models to examine terrestrial ecosystem responses to global change (Melillo et al. 1993, Cramer et al. 2001). However, the connections between climate, soil conditions, and vegetation dynamics are poorly understood and are highly simplified in most models.

Biogeochemistry models are quantitative representations of our understanding of the storage and transport of carbon, water and nutrients through soil, vegetation and the atmosphere. They incorporate nonlinearity of processes, and the multiple scales and interactions of processes. They generally operate in two-dimensional space and are typically run with hourly to daily climate data over years to centuries. A limitation of such process models is that they require mass and energy balance, sometimes at temporal and spatial scales that may not make sense relative to how processes actually occur. Mass and energy balance also cannot necessarily be quantified with field measurements to test model assumptions. For example, flux sites that measure ecosystem energy components have found that on average, they can only account for ~80% of net radiation (Wilson et al. 2002). As a result, models are often evaluated by comparison with measurable budget components (e.g., Law et al. 2001a).

Biogeochemistry models use input parameters for the physiology, biochemistry, structure, and allocation patterns of vegetation functional types, or biomes. For single-stand simulations it is possible to measure many of the required model parameters, but as spatial coverage increases, data availability decreases, and generalized biome parameterizations are applied. For example, parameterization may be simplified to constant foliar nitrogen across a biome or life form in a region using data from the literature. Similarly, allocation of carbon to plant tissues may be assigned as fixed fractions across age classes and climatic zones. Undocumented parameter selection and unknown model sensitivity to parameter variation for larger-resolution simulations are currently a major limitation to regional and global modeling (White and Running 1994, White et al. 2000). Although some ecosystem process models are dynamic and converge towards carbon, nitrogen and water balances, they can result in the right answer for the wrong reasons, or a predicted variable such as net primary productivity can be quite inaccurate because of a variety of uncertainties in model structure or parameters.

Decision rules are usually developed for selecting parameters in regional modeling. The procedure is usually to identify the simplest parameterizations (the default variables) and to then test the model to determine which parameters need more specification. Another method for parameterization is data assimilation, which has been used for a long time in atmospheric research, but it is relatively new to scaling ecosystem processes (e.g., Cescatti 1997). Data assimilation is the process of finding the model representation that is most consistent with the observations. Data assimilation usually proceeds sequentially in time. The model organizes and propagates forward the information from previous observations. Information from new observations is used to modify the model state, and to be as consistent with them and the previous observations (e.g., time series in Kalman filter, a Bayesian approach). As more data become available, such an approach may make sense for some parameters in regional carbon cycle scaling applications.

Another scaling issue is the mismatch of scales between observations and predictions. Model output variables include carbon storage in live and dead pools, net primary production (NPP), and net ecosystem production (NEP). Computational logistics and availability of spatial data for running the models may require simplifications that include linear aggregation of input and output variables. "Big leaf" models such as Biome-BGC assume a homogeneous 2-dimensional layer of foliage for resource use, carbon uptake and transpiration over a grid cell that can range from 30 m to 1 km to 0.5 degree (longitude and latitude) on a side. Evaluation of modeled NPP across a region is often conducted by comparing 1 km mean NPP values with 1 hectare means from tree structure measurements scaled by allometry, a mismatch in spatial scales when in reality, NPP may be heterogeneous within 1 km (e.g., clearcut and mature forests within 1 km; Turner et al. 2003). Temporal mismatches in scale also occur, whereby time-integration of available data and model output differ. Limited availability of field estimates of NPP or biomass across regions and continents has resulted in comparisons between model averages over years with field estimates over a variety of single or multiple years. The mismatch in time and space has uncertainties associated with it, yet this is difficult to quantify and overcome.

9.3 AN APPROACH TO SCALING AND UNCERTAINTY ANALYSIS OF ECOSYSTEM PROCESSES IN FORESTS – A CASE STUDY

The goal of the regional TERRA-PNW project is to estimate carbon storage, NPP and NEP for every square km of forest across a region over several climate years with improved accuracy, and explain sensitivity of NEP to cover type, forest age, disturbance, and interannual variability in climate. The approach is to spatially distribute a biogeochemistry model (Biome-BGC) which assimilates a wide range of spatially explicit information about the environment, using a combination of remote sensing and field observations as model input and for model testing. To treat the complexity of the carbon cycle, our modeling approach takes advantage of the near decomposability (*sensu* Wu 1999) of the ecological hierarchy (Table 9.1). At the level of the ecosystem, our emphasis is on NEP (annual time step). The associated

processes of photosynthesis and heterotrophic respiration are treated separately at the daily time step. At the ecosystem level, the key dynamic is the successional trend from negative NEP to positive NEP over multiple years. Because our emphasis here is primarily on annual NEP, we do not treat the longer time frames and processes relevant to interactions within holons at the upper levels of the hierarchy, e.g., interactions among age classes within a landscape mediated by fire, or interactions among ecoregions within a region mediated by climate change. However, differentiation of these upper levels remains useful because it permits specification of unique model parameterizations for ecophysiological constants such as specific leaf area (SLA).

Table 9.1. *Delineation of the ecological hierarchy.*

Level	*Examples*
Region	Pacific Northwest
Ecoregion	Coast Range, West Cascades
Landscape	Intensive Management, Wilderness
Ecosystem	Young, Mature, Old Growth Stands
Functional Group	Producers, Decomposers

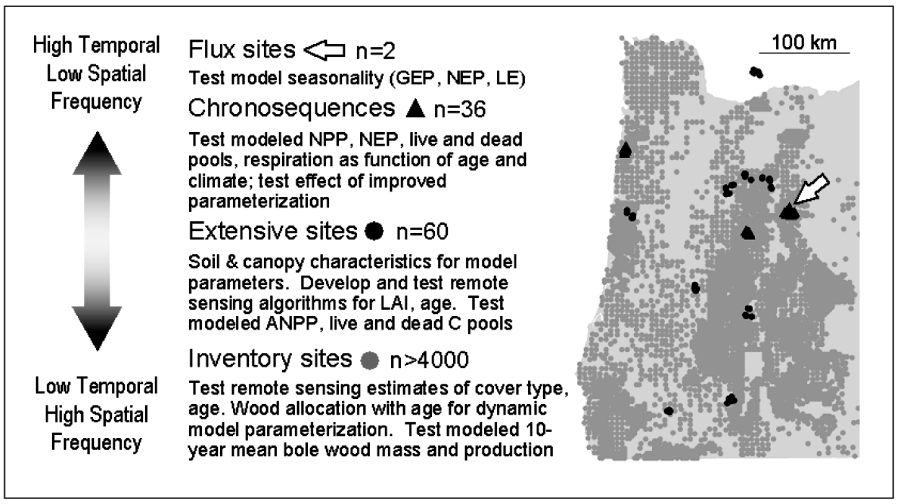

Figure 9.2. *Hierarchical approach to collecting the field data used to develop model parameters, develop remote sensing algorithms, and validate model output. Due to confidentially requirements, mapped locations are only approximate.*

Biome-BGC is fundamentally a daily time step model of coupled carbon, nitrogen, and water cycles (version 4.1.2; Thornton et al. 2002). It requires spatial data on land cover classification, stand age, and a reference leaf area index (LAI), all provided by satellite remote sensing, and it is driven with a distributed daily

climatology (DAYMET model). Model outputs included gross photosynthesis (GPP), net primary production (NPP of foliage, above- and belowground wood, fine roots), heterotrophic respiration (Rh) and NEP.

Model sensitivity tests are used to determine critical input variables to measure in the field for a range of forest types and developmental stages. White et al. (2000) conducted a sensitivity analysis with Biome-BGC and found that simulated NPP for all biomes is significantly affected by variation in foliar and fine root C:N, and NPP of woody biomes is strongly controlled by leaf nitrogen in Rubisco, maximum stomatal conductance, and SLA while non-woody biomes are sensitive to fire mortality and litter quality.

The scaling strategy is to use a spatially nested hierarchy (Wu 1999) to optimize field measurements for model parameters and testing. Field observations range from inventory data (many locations, few variables), to extensive sites, and intensive sites (chronosequences and tower flux sites, greater frequency and types of measurements, fewer locations) (Figure 9.2). Some field measurements are relatively easy to make, and are needed for the wide range of vegetation types and environmental conditions. For example, the model parameters foliar C:N and SLA can be measured at mid-season at many locations (extensive sites). More difficult measurements, such as stomatal conductance, are carried out at fewer intensive sites, or values are obtained from the literature. Remote sensing is a useful tool for obtaining spatially distributed vegetation characteristics (Wessman and Bateson, Chapter 8). A large pool of field data is required to develop and test remote sensing algorithms for vegetation mapping, so field observations are needed at many locations to cover the domain of application (e.g., LAI, forest type, and forest age at extensive sites).

To aid diagnostics, model outputs are evaluated with observations at a variety of spatial and temporal scales, starting with the most intensive observations and followed by more distributed sites that have less information. Then necessary improvements in model structure and parameters are identified and implemented, and model testing is reiterated at multiple scales.

We demonstrate the scaling approach over an east-west swath across central Oregon (300 km × 50 km) that covers a strong climatic gradient from the mild coastal conditions where water is not limiting to growth, to the Cascade Mountains where snowfall and freezing temperatures occur, to the semi-arid east side of the Cascade Mountains where temperatures are more continental (as in Figure 9.3).

9.4 FIELD OBSERVATIONS

9.4.1 Flux Sites: Measurements

Eddy covariance flux sites, such as the AmeriFlux network of sites (currently 80 sites in North, Central and South America) provide net CO_2 and water vapor exchange data. Flux systems comprise three-axis sonic anemometers that measured wind speed and virtual temperature, and infrared gas analyzers that measure concentrations of water vapor and CO_2 above the canopy. Fluxes are averaged half-hourly, and data are

evaluated for quality (Law et al. 2001a, Baldocchi 2003). Additional biological measurements typically made at the sites provide data for evaluating flux components (e.g., transpiration, respiration). Flux data are aggregated daily to examine seasonal trends in simulated and observed GPP, net ecosystem production (NEP), and latent energy flux (LE, evaporation and transpiration), and diagnose potential causes for discrepancies.

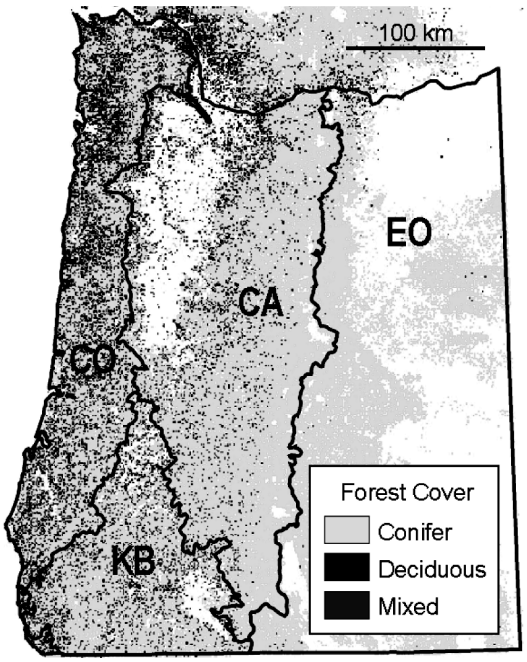

Figure 9.3. *Forest cover type map derived from remote sensing and supplementary GIS data. Grey lines denote ecoregions in each of which are recognized five forest classes (conifer, deciduous, mixed, semi-open, and open). Semi-open, and open together represent only 8% of the forested area and as such do not resolve on this figure.*

9.4.2 Flux Sites: Uncertainty Analysis

In previous studies (Anthoni et al. 1999) we quantified uncertainty in eddy flux estimates of NEP by combining systematic errors geometrically, and estimated that the overall uncertainty of the daytime carbon dioxide flux was ~±12% of the mean half-hourly flux. Nighttime fluxes are more problematic due to low wind conditions in tall canopies, and when data are screened to remove these periods, the cumulative error can result in substantial uncertainty in annual estimates of NEP. Therefore, the flux data are most useful for testing models when aggregated to a daily or monthly timestep, a range consistent with the time-step of Biome-BGC.

9.4.3 Chronosequence Plots: Measurements

To expand the range of forests types for which we had reliable estimates of NEP, 36 additional study plots were established across a strong precipitation gradient in the study region. The chronosequence plots are consist of 3 independent replicates of 4 age classes blocked by 3 forest types. Forest ages range from 10 to 300 years and are classified as either initiation, young, mature or old.

The mass balance approach we used to estimating NEP is:

$$NEP = (NPP_A - R_{WD}) + (\Delta C_{FR} + \Delta C_{CR} + \Delta C_{soil} - fine\ litterfall) \quad (9.1)$$

where NPP_A is aboveground net primary production (wood and foliage by both over- and understory plants), R_{WD} is the respiration from woody debris (decomposition of coarse and fine woody debris, stumps and snags), ΔC_{FR} is the net change in fine root C (not different from zero in this study), ΔC_{CR} is the difference between the net growth live coarse roots and the decomposition of coarse roots attached to stumps, ΔC_{soil} is the net change in mineral soil C (not different from zero in this study), and fine litterfall includes leaves and twigs <1 cm diameter falling to the ground in one year.

Procedures for measuring the components of equation 1 are detailed in Law et al. (2003) and generally rely on radial stem growth and allometric biomass equations for estimating woody production, optical measures of LAI and leaf turnover for estimating foliar production, volume inventory and decay functions for estimating dead wood respiration, and soil coring for estimating change in soil and fine root C.

9.4.4 Chronosequence Plots: Uncertainty Analysis

Both an experimental and measurement uncertainty was assessed for the NEP values (Table 9.2). For the purpose of describing the range of behavior exhibited by a certain condition class (forest type and age in this study) the most useful measure of uncertainty is an expression of the variance among true replicates of the condition, i.e., "experimental" uncertainty. This was calculated for all measured parameters, including NEP, simply as the standard deviation among the replicated plots (3 per age class). Computing the experimental uncertainty is appropriate only when there are true plot replicates (see Hurlbert 1984).

For the purposes of model validation, there is a desire to know the measurement error, which can stem from both the instrument error (e.g., calibration of carbon dioxide gas analyzer) and the error that arises from sample design (e.g., variation among soil cores used to estimate plot-level fine root mass). To assign measurement uncertainty to a composite parameter such as NEP, it is necessary to know the uncertainty associated with its components such as wood production or coarse woody debris decomposition. However, it is not possible or practical to account for all sources of uncertainty. For instance, measurement uncertainty exists in the coring of tree boles to determine their radial growth, however we know from prior analysis

that this error is insignificant compared to the extrapolation of these data to uncored trees on the same plot based on diameter-increment regressions. Consequently, the uncertainty in the radial increment component of NPP_A is based solely on the diameter-increment regressions.

Another example of using sampling error as the primary source of measurement error is in the assessment of plot-level LAI, which was measured with an LAI-2000 at 39 points regularly stratified throughout each plot. The standard deviation of these 39 measurements served as the plot-level uncertainty. Potentially, uncertainties in LAI could also be attributed to error in clumping corrections at both leaf and stand scale, but such errors are not quantifiable in practice. Fractional values of LAI (e.g., 0.5) make little difference biologically and in process modeling as indicated by model sensitivity tests (Thornton et al. 2002).

Table 9.2. *Means, experimental uncertainties, and measurement uncertainties for field estimates of aboveground net primary production (NPP_A), belowground net primary production (NPP_B), and net ecosystem production (NEP), for each age class and cover type represented by the chronosequence plots.*

	NPP_A ($gC\ m^{-2}\ yr^{-1}$)		NPP_B ($gC\ m^{-2}\ yr^{-1}$)		NEP ($gC\ m^{-2}\ yr^{-1}$)	
Cascade Head						
Initiation	793	(83, 22)*	273	(83, 95)	555	(95, 37)
Young	801	(26, 48)	259	(99, 73)	393	(104, 63)
Mature	657	(44, 59)	202	(22, 70)	423	(55, 73)
Old	486	(145, 49)	217	(68, 81)	238	(98, 71)
HJ Andrews						
Initiation	315	(24, 34)	252	(52, 118)	199	(23, 35)
Young	476	(127, 31)	234	(45, 66)	288	(115, 44)
Mature	478	(103, 40)	274	(74, 99)	314	(170, 54)
Old	318	(53, 56)	218	(34, 128)	–24	(148, 83)
Metolius						
Initiation	114	(42, 8)	94	(52, 43)	–129	(110, 17)
Young	231	(27, 19)	169	(47, 43)	117	(59, 31)
Mature	323	(151, 36)	162	(75, 62)	169	(200, 46)
Old	180	(71, 27)	152	(34, 45)	34	(121, 35)

** The first value in parentheses is the experimental uncertainty (1 SD of the mean of 3 replicate plots). The second value in parentheses is the average measurement uncertainty calculated for each site-age combination (measurement uncertainty determined for each plot by Monte Carlo simulation as 1 SD of 1000 standard normal iterations, accounting for covariance among equation components).*

Once an appropriate measurement uncertainty was assessed for each of the components of NEP (Equation 9.1), Monte Carlo simulations were used to determine a final aggregate uncertainty. By randomly sampling within the probable distribution of each variable (set by its own measurement uncertainty), a single

Monte Carlo run generates one probable value for NEP. Repeating the simulation 1000 times generates a distribution of probable NEP values. A final measurement uncertainty for NEP is expressed as the standard deviation of this distribution. In this study we assumed that uncertainty about each component of NEP had a standard normal distribution. When using Monte Carlo simulations it is important to consider the covariance among component variables. Some Monte Carlo models accommodate a correlation matrix that quantifies the covariance among equation components. A simpler alternative, employed here, was to combine equation components known to be computationally linked (such as understory wood and foliage mass which are both derived from stem diameter) into one variable before running the Monte Carlo simulation. In this study, experimental uncertainties in NEP averaged 44% and measurement uncertainties averaged 19% of the mean NEP, with the highest uncertainties in the oldest forests (Table 9.2).

9.4.5 Extensive Plots: Measurements

There is generally a large gap in field observations between the relatively low number of sites where it is feasible to make intensive measurements, and the large number of inventory sites where only a few measurements are made. To bridge this gap, we established 60 additional plots using a hierarchical random sample design that allowed maximum representation of forest types that exist in the region, the age classes present, and the climate space. A single visit to the plots provided data on soil and canopy C and N, maximum LAI, biomass and aboveground productivity for the range of environmental conditions and forest types. LAI measurements from these plots were used to develop the regressions that predicted LAI from remote imagery.

9.4.6 Extensive Plots: Uncertainty Analysis

Uncertainty computations for the extensive plots followed the same procedures described above for the intensive plots. The uncertainty in field estimates of NPP_A and live mass aboveground (LM_A) at the extensive plots averaged 8 and 9% of the means (1 SD), respectively.

9.4.7 FIA/CVS Inventory Plots: Measurements

Federal forest inventories are repeated on a large number of forested plots in Oregon that are visited relatively infrequently. Current Vegetation Survey (CVS) plots are on federal national forest lands (4468 CVS plots in Oregon) and Forest Inventory & Analysis plots (FIA) are on private lands (1120 plots). CVS and FIA sampling intervals are 10 and 8-12 years, respectively. The measurements made on these plots are primarily tree structural dimensions and species. These data are used to estimate biomass during each measurement period, and ~10-year mean stemwood production. Limited measurements of some variables, such as wood increment (33% of trees) and tree height (23% of trees), reduce confidence in the accuracy of the estimates of

biomass and productivity but remain valuable since the large number of plots can be used to evaluate trends in stemwood biomass and growth across climatic zones and forest types, and to determine relative accuracy of model predictions in these different conditions. For the inventory plots, stemwood mass was calculated from

$$Biomass_b = Volume_b \times Wood\ Density \tag{9.2}$$

where $Volume_b$ is stemwood volume, and wood density is the dry density of wood.

The ~10 year mean NPP of aboveground stemwood was estimated from

$$NPP_{Aw} = Biomass_{w2} - Biomass_{w1} \tag{9.3}$$

Where NPP_{Aw} is aboveground NPP of stemwood and $Biomass_{w2}$ and $Biomass_{w1}$ are aboveground woody biomass at current and previous time steps, respectively. Previous and current height of unmeasured trees was modeled using height-diameter equations developed in the region from forest inventory data (Garman et al. 1995). The study area was divided into four geographic regions, each corresponding to commonly acknowledged physiographic zones in Oregon (Oregon Coast Range, Western Cascades, and Eastern Cascades – after Franklin and Dyrness 1973). When possible, physiographic zone and species-specific allometric equations were applied to estimate volume. Wood density data were acquired for most of the major hardwood and softwood species of western Oregon through wood density surveys conducted by the U.S. Forest Service (USDA Forest Service 1965, Maeglin and Wahlgren 1972).

9.4.8 FIA/CVS Inventory Plots: Uncertainty Analysis

Error estimates for NPP_{Aw} are based on uncertainty in radial growth propagated through the allometric models. In Van Tuyl et al. (2005), we made estimates of the potential magnitude of error associated with using generic wood densities and non-site specific allometry. The error associated with using generic versus plot-specific wood densities on 36 plots was estimated to be about 10%. An empirical comparison of volume equations used in this study suggests that errors as high as 40% of the mean could result from using equations not developed in the study area. These results suggest that site-specific volume allometry is much more important to making quality estimates of biomass and NPP than are site-specific wood density.

9.5 REMOTE SENSING OBSERVATIONS

The role of remote sensing in this study, as in many regional studies, is to provide large-domain spatial data layers that the biogeochemistry process model requires: LAI, stand age, and forest type. In particular, the prediction of stand age throughout this ecologically diverse region required different approaches in different stand types. While reasonable continuous estimates of stand age have been made using remote sensing of closed-canopy Douglas-fir/western hemlock forests in western

Oregon (Cohen et al. 2001), similar efforts in the open forests east of the Cascade Mountains were met with only limited success. Therefore, questions of scaling over these varying stand types must inherently address the varying data precisions in each area.

9.5.1 Land Cover

Forest cover for the study area was created by updating the 1988 forest cover layer created by Cohen et al. (2001) using the same land cover classes (Table 9.3). Non-forest areas (primarily urban and agricultural areas totaling 24% of land area) were defined using masks taken from Cohen et al. (2001) and supplemented with information from the National Land Cover Database (NLCD) for the eastern portion of the study area (Vogelmann 1998). For the purposes of this study, all forested areas in the East Cascades ecoregion were considered closed coniferous forest, and their extent was fixed by the NLCD coverage. Of over 8.8 million hectares of forest, 3% was in an open condition, 8% was semi-open, 5.5% was deciduous, and 16% was mixed forest (Figure 9.3). The resulting land cover information was validated using 24 aerial photos distributed throughout the western study area, with an average accuracy of 82%, and a range of 49% to 97%.

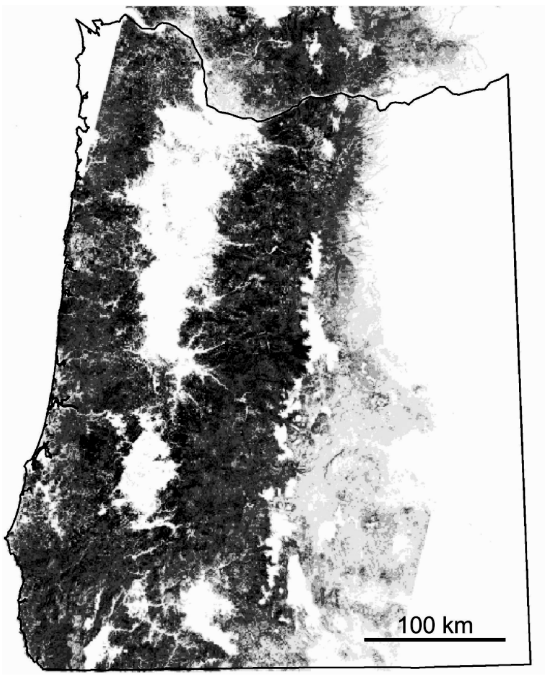

Figure 9.4. *Leaf area index (LAI) map derived from Landsat EMT+.*

9.5.2 Forest Age

The date of stand replacing disturbance can serve as a surrogate for stand age, with the caveat that stand re-establishment periods can vary according to resource availability and competition for resources (e.g., Law et al. 2003). To increase the accuracy of the estimates of age in the earliest stages of forest succession (when carbon flux changes rapidly), the continuous estimates of stand age were combined with age estimates based on mapping of disturbance through change detection.

A map of forest age was created by using an existing 1988 dataset of Cohen et al. (2001) extending it to the east side of the Cascade Mountains. It was updated to reflect age in Year 2000, and masked to remove areas that had changed since 1988. Regression between the 2000 tasseled-cap image and the ages in 1988 were used to estimate the remaining ages needed for new conifer areas. This relationship explained 68% of variance of log-transformed age, with an RMS residual of 0.392 log-years, which were similar to the 65.9% of variance and 0.592 RMS residual of 0.57 reported by Cohen et al. (2001).

Table 9.3. *Forest cover definitions for remote sensing land cover classification.*

Cover Class	*Definition*
Non-forest	Forested Cover < 0
Open	Total Forest Cover < 30%
Semi-open	30% < Total Forest Cover < 70%
Deciduous	Total Cover > 70% and Conifer Cover < 30%
Mixed	Total Cover > 70% and 30% < Conifer Cover < 70%
Conifer	Total Cover and Conifer Cover > 70%

9.5.3 Leaf Area Index

The remote sensing estimates of leaf area index (LAI) ranged from 1 to 12 in the West Cascades and Coast Range, and 0.5 to 8 in the East Cascades (Figure 9.4). To construct LAI algorithms, LAI was measured at the 96 extensive and intensive plots following methods in Law et al. (2001b). Polygons were hand digitized around each of the plots in reference to the Landsat ETM+ scene to ensure that a homogenous region was being referenced in the comparison of spectral characteristics and LAI. Both the tasseled-cap index and NDVI indices were calculated from the ETM+ mosaic and stepwise multiple regressions were used to determine the best set of variables for predicting LAI. The resulting equation uses brightness raised to the second power and wetness raised to the power of 11.606, explains 80% of variance, and has an RMSE of 1.668 (Figure 9.5). Subsequent analysis of the residuals for the East Cascades ecoregion indicated that LAI in those plots was underestimated by ~20%. Using a combined data set of 24 plots collected in 1999 and 2001, a new coverage was calculated for the East Cascades. The resulting equation uses only the wetness variable, raised to the power of 14.876, explains 82% of variance and has an RMSE of 0.742 (Figure 9.5). Both equations explain similar percentages of

variance, but the RMSE for the East Cascades is lower, probably due to the lower number of observations in this ecoregion.

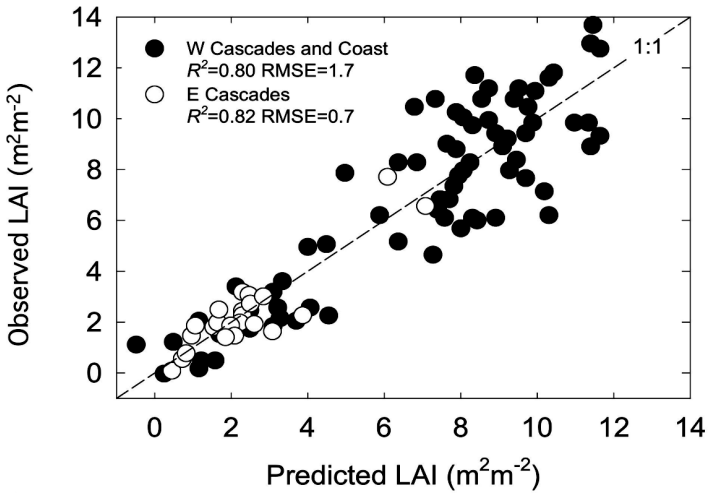

Figure 9.5. *Predicted and observed leaf area index (LAI) for field plots in the Eastern Cascades and combined plots of the Coast Range and Western Cascades.*

9.6 IMPLEMENTATION OF THE DISTRIBUTED MODELING

9.6.1 Overview

The Biome-BGC model (Thornton 1998, Thornton et al. 2002) was selected for this application because it includes the complete carbon cycle, it can assimilate input data from multiple sources (notably plot level measurements of parameters such as foliar nitrogen concentration), and it disaggregates carbon cycle processes sufficiently enough to allow comparisons with a wide variety of observations. The model has been previously tested at individual plots in coniferous forests of the PNW region (Running 1994, Law et al. 2001a).

Biome-BGC was run on a 25 m grid covering most of Oregon west of the Cascade Mountains. Much of the forested portion of the Pacific Northwest is characterized by clearcut patches smaller than 1 km^2 (Cohen et al. 2002), so high spatial resolution is essential to characterize spatial patterns in carbon flux (Cohen et al. 1996, Turner et al. 2000). Conversely, a 1 km resolution is suitable to capture much of the significant variation in climatic variables.

9.6.2 Climate Inputs

For climate inputs, Biome-BGC requires daily estimates of minimum and maximum temperature, precipitation, vapor pressure deficit, and solar radiation. A daily time

step, 1-km grid for these variables over the period of 1980-1997 was used in this application. This data set was generated by interpolation of meteorological station data using the DAYMET program (Thornton et al. 1997, Thornton and Running 1999, Thornton et al. 2000).

9.6.3 Model Spinup

Biome-BGC was specifically designed to simulate changes in carbon fluxes over long periods. The model must therefore be run over a 1000+ year "spinup" to bring the slow turnover soil carbon pools into near steady state. Disturbances such as clearcut harvests are then imposed, accounting for tree carbon affected by the disturbance. For each model run in this analysis, two successive disturbances separated by 60-90 years (depending on location) were simulated at the end of each spin-up such that 1/3 of the live tree carbon was transferred to the coarse woody debris pool at each disturbance. The model was then run forward to the age specified by the remote sensing classification. The 18-year climate time series was run repeatedly in these analyses and manipulated such that the last year of secondary succession was always 1997.

9.6.4 LAI Optimization

LAI is prognostic in BIOME-BGC, and although LAI can be remotely sensed, it cannot simply be prescribed in the model because of the continuous interaction among the various model compartments. Earlier analysis in Pacific Northwest conifer stands has shown a strong linear relationship between stand LAI and a site water balance index based on annual precipitation, annual potential evapo-transpiration, and soil water holding capacity (Grier and Running 1977). To achieve agreement between remotely sensed LAI and simulated LAI for a given cell in this application, a secant method (Cheney and Kincaid 1985) was used with model runs at different soil depths to iteratively solve for the soil depth that minimizes the difference between a reference LAI (e.g., from remote sensing) and simulated LAI at a specified stand age. An initial value of soil depth to seed the iterations was taken from a digital map of soil depths based on the State Soil Geographic (STATSGO) database (Kern et al. 1997). In young stands that may not have achieved equilibrium LAI, the minimum possible soil depth was constrained by the distribution of STATSGO soil depths in the ecoregion. Using this approach, the fit between remotely sensed LAI and Biome-BGC LAI was good ($r^2 = 0.97$) with an RMSE of 0.5 LAI units.

9.6.5 Integrating 1 km and 30 m Data

A critical issue in the distributed model implementation was the scale mismatch between land cover and LAI data at the 25 m resolution and the climate data at 1 km resolution. Because of computational constraints associated with the model spinups, a unique model run could not be made at each 25 m cell in the region of interest.

Thus, a separate model run was made only once in each 1 km cell for each combination of cover type and age class. For use in the soil depth determination, a reference LAI was determined for each cover type × age class combination within each 1 km cell. The remotely sensed reference LAI was the mean for all 25 m cells belonging to each cover type × age class combination within the 1 km cell.

9.6.6 Ecophysiological Inputs

Biome-BGC requires a set of ecophysiological constants for model initialization. We created a generic set of constants for each cover type based on the values in White et al. (2000). The White et al. (2000) analysis determined that the model was particularly sensitive to values of foliar C:N and SLA, so we also created ecoregion-specific sets of constants where foliar C:N and SLA values were means based on field measurements at the intensive and the chronosequence plots.

9.6.7 Comparisons of Simulations with the Survey Data

The comparison of simulated stemwood production with observations from the FIA survey data was constrained by a number of factors. Besides the initial problem of converting information on distributions of diameter and growth increment into wood production, these factors included (1) plot location, (2) convergence of model output and inventory data on a common parameter, and (3) achieving overlap in time between the observations and the simulations.

Perhaps the most significant issue for model evaluation inaccuracy in some plot locations. Federal law currently prohibits release of FIA plot locations for both private and public lands (recent amendment of the Food Security Act). Thus, researchers outside of the FIA program are extremely limited in their ability to conduct analyses of the data in a spatial context. In addition, locations of the CVS plots on public land were not determined with Global Positioning Systems, so the locations are somewhat uncertain.

Because much of the forested land in the study area is publicly owned, the set of CVS plots was used for the purposes of comparing survey-based and simulated wood production. CVS locations were accepted as reported and the coordinates were used to determine an associated 1 km cell within the climate grid. In the model spinups used to determine soil depth, the reference LAI was the mean value for all 25 m cells in the relevant cover class within the 1 km cell. After the soil depth was selected, the model spinup completed, and the disturbances imposed, the model was run to the age specified by the CVS data.

The problem with temporal overlap in the CVS and simulated data is caused by the nonuniformity in the year of visit to the permanent plots, and the observation that there is large interannual variation in bolewood production based on climate variation in the Pacific Northwest (Turner et al. 2003). CVS plots are visited on a roughly 10-year interval, and the growth increment is reported for the previous 10 years. There are also delays in getting the data into the FIA database. Thus data at the time it was received from FIA (in the year 2001) may have been five or more

years old. The model NPP_{Aw} can be aggregated over any interval desired, and for this study the mean NPP_{Aw} over the 10 yr period from 1988-1997 was selected for the comparisons. Because of the many constraints on achieving a implemented in this Biome-BGC application such that allocation to fine roots and leaves one-to-one comparison in space and time between the CVS data and the simulation data, comparisons were made more generally by examining relationships of NPP_{Aw} to stand age within the ecoregions.

An age-specific allocation scheme was increased in older stands, except those of the East Cascades ecoregion where empirical data indicated that allocation to fine roots is greater in young stands (Law et al. 2003). The ecological rationale for increased root and leaf allocation with age follows the nutrient limitation hypothesis, i.e., nutrients become more limited in late succession because they are increasingly sequestered in the biomass. Allocation to fine roots thus increases, and correspondingly stemwood production decreases. This is not an appropriate rationale for water-limited ecosystems, where relatively large allocation to roots throughout stand development is critical for survival.

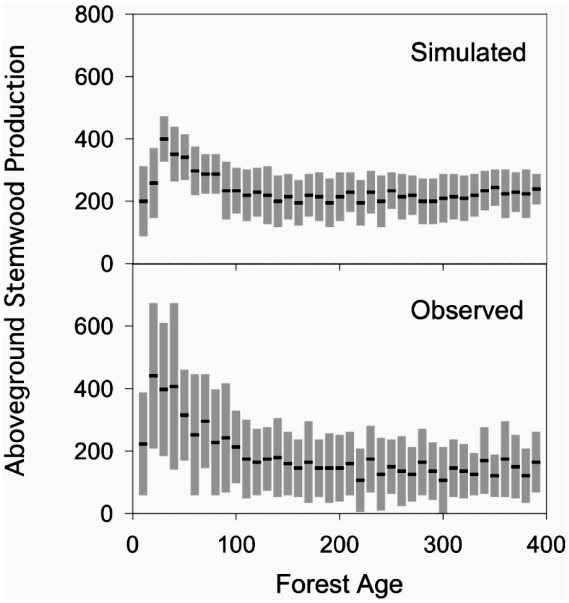

Figure 9.6. *Simulated and observed aboveground stemwood production in relation to stand age for the West Cascades CVS inventory plots. Grey bars are the standard deviation of 6 to 36 plots depending on age class.*

To implement the allocation shift in the model simulations for the Coast Range and West Cascades ecoregions, a nonlinear increase in the allocation to leaves and fine roots was prescribed in late succession. The relevant parameters were a maximum stemwood production rate in young stands, a lower stable stemwood

production rate in older stands, and an age that indicated the midpoint of the transfer. These parameters were based on a cubic polynomial fit to the CVS NPP_{Aw} data by ecoregion (Figure 9.6). With the dynamic allocation implemented in the model, the ratio of NPP_{Aw} in old and young stands came into much closer agreement with the observations (Table 9.4).

Table 9.4. *Model/data comparisons (CVS plot data) for the ratio of aboveground net primary production for wood (NPP_{Aw}) at the low and high extreme points of the cubic polynomial fit for NPP_{Aw} versus forest age. Units are g C m^{-2} y^{-1}. N is the number of observations, CI is the 95% confidence interval for the predictions at the forest ages corresponding to the high (young) and low (old) extremes of the fitted cubic polynomial model.*

	N	*Ratio*	*Young*	*CI*	*Old*	*CI*
Observations						
Coast Range	383	0.50	705	272 -1137	354	–64 - 772
West Cascades	1677	0.44	469	214 - 724	208	–45 - 462
Model-Before Dynamic Allocation						
Coast Range	373	0.92	353	263 - 443	324	243 - 413
West Cascades	1626	0.86	330	182 - 477	285	138 - 432
Model-After Dynamic Allocation						
Coast Range	373	0.69	456	353 - 559	314	211 - 416
West Cascades	1626	0.51	366	235 - 497	185	55 - 315

Across all ecoregions, the model NPP_{Aw} values were similar to the CVS data in that the highest magnitudes were in the Coast Range ecoregion, slightly lower values in the West Cascades ecoregion, and much lower values in the East Cascades. There was generally more scatter in the CVS observations than in the simulations. This may occur in part because of a tendency for the scaling approach to under-represent sites with low and high LAI (due to the necessity of averaging LAI within each cover class by age class combination over the 1 km grid cells). The permanent plot data will be further utilized for model improvement by examining the relationships of NPP_{Aw} to climate indices such as annual potential evapotranspiration, and evaluating the degree to which the model is responding in a similar fashion.

9.6.8 Comparisons of Simulations with the Extensive Plot Data

Comparisons were made between observations and modeled NPP_{Aw}, total aboveground NPP (NPP_A), and stem mass at the 96 extensive plots (including the intensive chronosequence plots). The model was run with the same protocols as for the CVS plots but used field observations of LAI as the reference LAI in determining soil depth. The comparisons (Table 9.5) showed good agreement for

NPP_{Aw} and NPP_A, but a tendency for the model to underestimate stem mass at older stand ages. A potential cause of stem mass underestimation is overestimation of tree mortality and those relationships are being explored with model sensitivity analyses and with evaluation of mortality estimates in the literature.

Table 9.5. *Regression statistics (observed vs. modeled) for extensive plot and chronosequence plot comparisons (b = slope and a = intercept). Flux units are g C m^{-2} y^{-1}, mass units are g C m^{-2}. See text for NPP abbreviations.*

Variable	*a*	*SE*	*b*	*SE*	R^2	*RMSE*
Extensive Plots (N=75)						
NPP_{Aw}	90	26	0.80	0.08	0.59	116
NPP_A	59	32	0.93	0.06	0.75	121
LM_{Aw}	3770	863	0.57	0.04	0.74	8950
Chronosequence Plots (N=36)						
NPP_{Aw}	62	31	0.81	0.09	0.69	100
NPP_A	36	37	0.93	0.08	0.82	103
NPP	20	79	1.10	0.11	0.73	207
LM_{Aw}	4240	1210	0.54	0.05	0.76	9630
NEP	99	38	0.55	0.12	0.37	183

Table 9.6. *Effects of alternative parameterization schemes on regression statistics for comparison of observed and modeled aboveground net primary production (NPP_A; b = slope and a = intercept). In the default case, all sites were run with the same set of ecophysiological constants. In the ecoregion case, there was a unique parameterization of the ecophysiological constants for each ecoregion, and in the site-specific case, there was a unique parameterization for each site.*

Parameterization	*a*	*SE*	*b*	*SE*	R^2	*RMSE*
Default	107	36	0.92	0.07	0.70	148
Ecoregion	49	33	0.94	0.06	0.75	121
Site Specific	63	41	0.89	0.08	0.63	150

To reveal the benefits of using the ecoregion-specific observations of foliar N concentration, SLA, and leaf retention, a comparison of observed and modeled NPP_A was also made for a model run using a generic conifer parameterization. Without the ecoregion parameterization, the model produced significant additive bias, and the RMSE was considerably higher (Table 9.6). The use of even more specialized (site-specific) values of foliar N, SLA, and leaf retention also showed improved fit over the generic conifer parameterization, but the RMSE was just as high due to large model error at a few sites. For each parameterization scheme, regressions of model-error against climate indices such as annual precipitation and summer precipitation were weak at best, except for the site-specific parameterization scheme. Possibly, other parameters linked to foliar C:N and SLA must be changed in parallel to achieve consistent improvements. Further analyses of these model errors in relation to climatic gradients may be helpful for diagnostic purposes.

9.6.9 Comparisons of Simulations with Chronosequence Data

At the chronosequence plots, comparisons were made between field-based and modeled NPP_{Aw}, NPP_A, total NPP, stem mass, and NEP (Table 9.5, Figure 9.7). The agreement between model and observations was best for NPP_A and NPP. For other variables the correlations were positive (with regression slopes >0.5), but further work on model development is needed. Future work will focus on the mortality parameter and on components of heterotrophic respiration, which strongly influence modeled NEP.

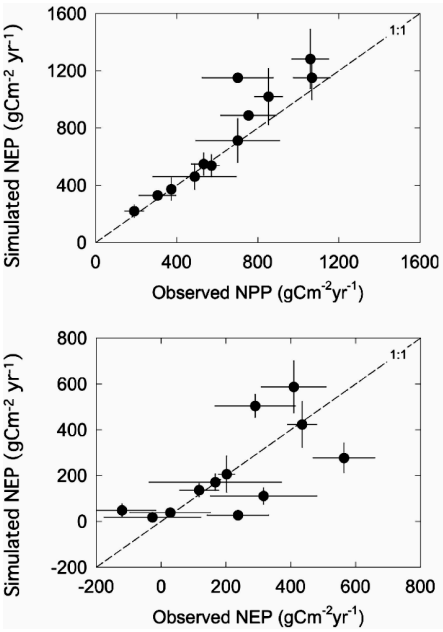

Figure 9.7. *Simulated and observed net primary production (NPP) and net ecosystem production (NEP) for the chronosequence study plots. Values are means and standard deviation of 3 replicate plots per site × age class combination.*

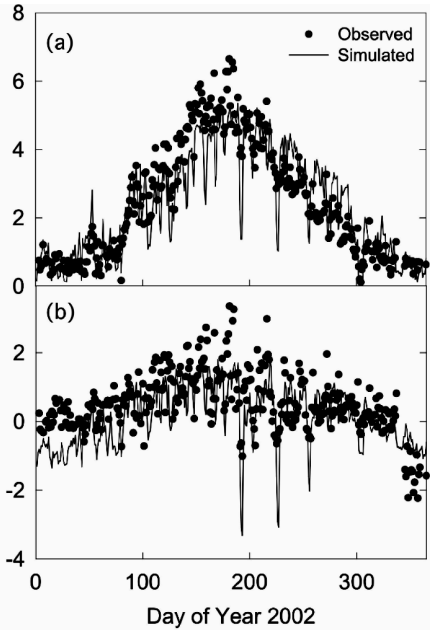

Figure 9.8. *Comparison of flux tower observations and model simulations of gross primary production (GPP) and net ecosystem production (NEP) at the Metolius young ponderosa pine site in 2002.*

9.6.10 Comparisons of Simulations with Flux Tower Data

Flux tower estimates of evapotranspiration were initially used to evaluate the generic parameterization derived from White et al. (2000). In examining observed and modeled evapotranspiration, it became evident that the default maximum stomatal conductance parameter was too high, and it was therefore reduced significantly. For the year 2001 comparisons, the time series plots of daily GPP at the young pine tower site suggested a slight underestimation of GPP in mid-growing

season (Figure 9.8). The model also consistently underestimated NEP throughout most of the growing season. There remain significant uncertainties in the nighttime NEE estimates from the tower data and the modeled NEE is the small net of the large GPP and heterotrophic respiration (errors in both). Thus, the comparisons must be considered tentative. Comparisons will be made with results of continuing efforts to quantify heterotrophic respiration fluxes in the field (Law et al. 2001a, 2003).

9.6.11 NEP Surfaces

After completion of model testing and parameterization based on the complete suite of observational data, the model will be run wall-to-wall over the east-west swath in western Oregon. Preliminary test areas in the three ecoregions (e.g., Figure 9.9) show the effects of management and environmental gradients. NEP is relatively low in areas recently clearcut for harvest, and highest in young stands (age 30-100) that have a closed canopy and have lost most residues from their stand-originating disturbance. NEP on the drier east side of the Cascades tends to be relatively low. Besides analysis of within region heterogeneity in NEP, the remote sensing/ modeling scaling approach will also permit analysis of interannual variation in NEP (Turner et al. 2003).

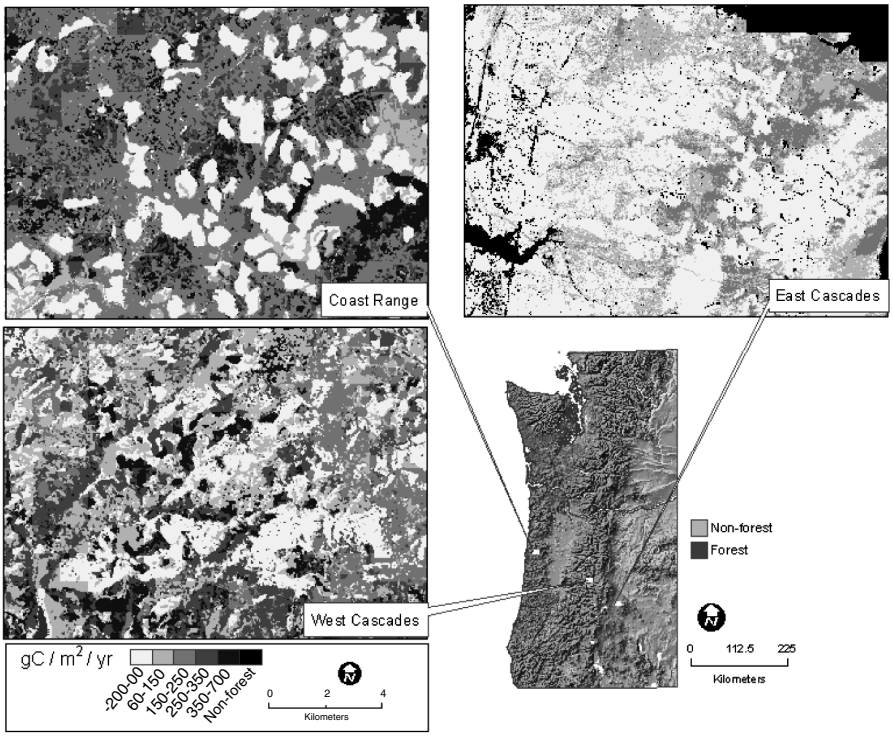

Figure 9.9. *Simulated net ecosystem production (NEP) for selected areas in the study region.*

9.7 CONCLUSIONS

Scaling in space and time is essential if we are to address global change issues relevant to terrestrial carbon cycling. We demonstrated a scaling strategy that uses a spatially nested hierarchy of observations for model parameterization and testing, along with a simulation model that provides a means of integrating environmental information at a range of spatial and temporal scales. Observations that include flux towers, intensive field sites, and inventory data increase understanding of ecological processes and permit the iterative process of model testing and improvement, recognizing there are uncertainties in field observations as well as model estimates. Uncertainty estimates for field observations, that are aggregates of multiple measurements, can be calculated by determining upper and lower boundaries for each component measurement and propagating these estimates through to a single variable (NEP in this case) with Monte Carlo models. Field observations over a range of environmental conditions are necessary for accuracy assessment of remote sensing estimates of vegetation characteristics. Knowledge of model sensitivities to key parameters helps to determine measurements that should be made at inventory sites (e.g., wood increment and density), extensive sites (e.g., foliar and soil carbon and nitrogen), and intensive sites (e.g., A-Ci curves – photosynthetic response to internal CO_2). In coniferous forests of the Pacific Northwest, disturbance history and environmental gradients are the major controls on carbon pools and fluxes. Thus, for regional analysis of carbon, nitrogen and water cycling it is critical to have spatial data layers such as remotely sensed estimates of cover type, changes in cover or disturbance, and spatially distributed climate. Advancements of the approach might include more iterative model development and testing and data assimilation techniques.

ACKNOWLEDGEMENTS

This study was funded by U.S. EPA - Science to Achieve Results (STAR) Program (Grant # R-82830901-0) and the Department of Energy (Grant # FG0300ER63014). Thanks to Peter Anthoni and Meredith Kurpius for tower flux data analysis, and to the following people for field data collection and analysis: Jesse Bablove, Jason Barker, Aaron Domingues, David Dreher, Marie Ducharme, Chris Dunham, Colin Edgar, Isaac Emery, Nathan Gehres, Angie Hofhine, Julie Horowitz, Nicole Lang, Erica Lyman-Holt, Darrin Moore, Adam Pfleeger, Lucia Reithmaier, Jennifer Sadlish, Matthew Shepherd, Nathan Strauss, and Vernon Wolf.

REFERENCES

Aber, J. D., C. Driscoll, C. A. Federer, R. Lathrop, G. Lovett, J. M. Melillo, P. Steudler, and J. Vogelmann. 1993. A strategy for the regional analysis of the effects of physical and chemical climate change on biogeochemical cycles in northeastern (U.S.) forests. Ecological Modeling 67: 37-47.

Anthoni, P. M., B. E. Law, and M. H. Unsworth. 1999. Carbon and water vapor exchange of an open-canopied ponderosa pine ecosystem. Agricultural and Forest Meteorology 95:151-168.

Baldocchi, D. D. 2003. Assessing ecosystem carbon balance: problems and prospects of the eddy covariance technique. Global Change Biology 9:479-492.

Cescatti, A. 1997. Modelling the radiative transfer in discontinuous canopies of asymmetric crowns. II. Model testing and application in a Norway spruce stand. Ecological Modelling 101:275-284.

Cheney, W., and D. Kincaid. 1985. Numerical Mathematics and Computing. Brooks/Cole, Monterey CA.

Cohen, W. B., M. E. Harmon, D. O. Wallin, and M. Fiorella. 1996. Two decades of carbon flux from forests of the Pacific Northwest. BioScience 46:836-844.

Cohen, W. B., T. K. Maiersperger, T. A. Spies, and D. R. Oetter. 2001. Modeling forest cover attributes as continuous variables in a regional context with Thematic Mapper data. International Journal of Remote Sensing 22:2279-2310.

Cohen W. B., T. A. Spies, R. J. Alig, D. R. Oetter, T. K. Maiersperger, and M. Fiorella. 2002. Characterizing 23 years (1972-1995) of stand replacement disturbance in western Oregon forests with Landsat imagery. Ecosystems 5:122-137.

Cramer, W., A. Bondeau, F. I. Woodward, I. C. Prentice, R. A. Betts, V. Brovkin, P. M. Cox, V. Fisher, J. A. Foley, A. D. Friend, C. Kucharik, M. R. Lomas, N. Ramankutty, S. Sitch, B. Smith, A. White, and C. Young-Molling. 2001. Global response of terrestrial ecosystem structure and function to CO_2 and climate change results from six dynamic global vegetation models. Global Change Biology 7:357-373.

Ehleringer, J. R., and C. Field, editors. 1993. Scaling Physiological Processes: Leaf to Globe. Academic Press, Orlando, FL.

Franklin, J. F., and C. T. Dyrness. 1973. Natural Vegetation of Oregon and Washington. Pacific Northwest Forest and Range Experiment Station. USDA Forest Service General Technical Report PNW-8.

Garman, S. L., S. A. Acker, J. L. Ohmann, and T. A. Spies. 1995. Asymptotic Height-diameter Equations for Twenty-four Tree Species in Western Oregon. Research Contribution 10. Forest Research Laboratory, Oregon State University, Corvallis, OR.

Grier, C. C., and S. R. Running. 1977. Leaf area of mature northwestern coniferous forests: relation to site water balance. Ecology 58:893-899.

Hurlbert, S. H. 1984. Pseudoreplication and the design of ecological field experiments. Ecological Monographs 54:187-211.

Jarvis, P. G. 1995. Scaling processes and problems. Plant, Cell and Environment 18:1079-1089.

Kern, J. S., D. P. Turner, and R. F. Dodson. 1997. Spatial patterns in soil organic carbon pool size in the Northwestern United States. Pages 29-43 *in* R. Lal, J. M. Kimbal, R. Follett, and B. A. Stewart, editors. Soil Processes and the Carbon Cycle. CRC Press, Boca Raton, FL.

Law, B. E., O. J. Sun, J. Campbell, S. Van Tuyl, and P. Thornton. 2003. Changes in carbon storage and fluxes in a chronosequence of ponderosa pine. Global Change Biology 9:510-524.

Law, B. E., P. Thornton, J. Irvine, S. Van Tuyl, and P. M. Anthoni. 2001a. Carbon storage and fluxes in ponderosa pine forests at different developmental stages. Global Change Biology 7:755-777.

Law, B. E., S. Van Tuyl, A. Cescatti, and D. D. Baldocchi. 2001b. Estimation of leaf area index in open-canopy ponderosa pine forests at different successional stages and management regimes in Oregon. Agricultural and Forest Meteorology 108:1-14.

Maeglin, R. R., and H. E. Wahlgren. 1972. Western Wood Density Survey: Report Number 2. USDA Forest Service Research Paper FPL-183.

Melillo, J. M., A. D. McGuire, D. W. Kicklighter, B. Moore, C. J. Vorosmarty, and A. L. Schloss. 1993. Global climate change and terrestrial net primary production. Nature 363:234-240.

Reich, P. B., M. B. Walters, and D. S. Ellsworth. 1997. From tropics to tundra: global convergence in plant functioning. Proceedings of the National Academy of Science 94:13730-13734.

Running, S. W. 1994. Testing FOREST-BGC ecosystem process simulations across a climatic gradient in Oregon. Ecological Applications 4:238-247.

Thornton, P. E. 1998. Regional ecosystem simulation: combining surface- and satellite-based observations to study linkages between terrestrial energy and mass budgets. Ph.D. Dissertation. School of Forestry, University of Montana, Missoula, MT.

Thornton, P. E., and S. W. Running. 1999. An improved algorithm for estimating incident daily solar radiation from measurements of temperature, humidity, and precipitation. Agricultural and Forest Meteorology 93:211-228.

Thornton, P. E., H. Hasenauer, and M. A. White. 2000. Simultaneous estimation of daily solar radiation and humidity from observed temperature and precipitation: an application over complex terrain in Austria. Agricultural and Forest Meteorology 104:255-271.

Thornton, P., B. E. Law, D. A. Ellsworth, H. Gholz, A. Goldstein, D. Hollinger, and K. T. Paw U. 2002. Modeling the effects of disturbance history and climate on carbon and water budgets in evergreen needleleaf forests. Agricultural and Forest Meteorology 113:185-222.

Thornton, P. E., S. W. Running, and M. A. White. 1997. Generating surfaces of daily meteorological variables over large regions of complex terrain. Journal of Hydrology 190:214-251.

Turner, D. P., W. B. Cohen, and R. E. Kennedy. 2000. Alternative spatial resolutions and estimation of carbon flux over a managed forest landscape in western Oregon. Landscape. Ecology 15:441-452.

Turner, D. P., M. Guzy, M. Lefsky, S. Van Tuyl, O. Sun, C. Daly, and B. E. Law. 2003. Effects of land use and fine scale environmental heterogeneity on net ecosystem production over a temperate coniferous forest landscape. Tellus 55B:657-668.

U.S. Department of Agriculture, Forest Service. 2001. Forest Inventory And Analysis National Core Field Guide, Volume 1: Field Data Collection Procedures for Phase 2 Plots, Version 1.5. Internal Report U.S. Department of Agriculture, Forest Service, Forest Inventory and Analysis, Washington, D.C.

Van Tuyl, S., B. E. Law, D. Turner, and A. Gitelman. 2005. Variability in net primary production and carbon storage in biomass across Oregon forests – an assessment integrating data from forest inventories, intensive sites, and remote sensing. Forest Ecology and Management 209:273-291.

Vitousek, P. M., J. D. Aber, R. W. Howarth, G. E. Likens, P. A. Matson, D. W. Schindler, W. H. Schlesinger, and D. Tilman. 1997. Human alteration of the blobal nitrogen cycle: sources and consequences. Ecological Applications 7:737-750.

Vogelmann, J., T. Sohl, and S. Howard. 1998. Regional characterization of land cover using multiple sources of data. Photogrammetric Engineering and Remote Sensing 64:45-57.

White, J. D., P. Thornton, S. W. Running, and R. Nemani. 2000. Parameterization and Sensitivity Analysis of the Biome-BGC Terrestrial Ecosystem Model: Net Primary Production Controls. Earth Interaction 4, paper No. 3.

White, M. A., and S. W. Running. 1994. Testing scale dependent assumptions in regional ecosystem simulations. Journal of Vegetation Science 5:687-702.

Wilson, K., D. D. Baldocchi, E. Falge, M. Aubinet, P. Berbigier, C. Bernhofer, H. Dolman, C. Field, A. Goldstein, A. Granier, D. Hollinger, G. Katul, B. E. Law, T. Meyers, J. Moncrieff, R. Monson, J. Tenhunen, R. Valentini, S. Verma, and S. Wofsy. 2002. The diurnal centroid of ecosystem energy and carbon fluxes at FLUXNET sites. Agricultural and Forest Meteorology 113:223-243.

Wu, J. 1999. Hierarch and scaling: extrapolation information along a scaling ladder. Canadian Journal of Remote Sensing 25:367-380.